μSR study of stoichiometric $NbFe_2$

D. Margineda[a], J.A. Duffy[b], J.W. Taylor[c], S.R. Giblin[a]

[a] *School of Physics and Astronomy, Cardiff University, Cardiff, CF24 3AA, United Kingdom*
[b] *Department of Physics, University of Warwick, Coventry, CV4 7AL, United Kingdom*
[c] *DMSC - European Spallation Source, Universitetsparken 1, Copenhagen 2100, Denmark*

Abstract

The magnetic ground state of nominally stoichiometric single crystalline $NbFe_2$ is investigated by bulk magnetisation and muon spin relaxation techniques. Magnetic order clearly emerges below the critical temperature T_N=10.3 K and is dominated by randomly orientated quasi-static moments. The local field distribution observed by muons can be explained by the phenomenological Gaussian-broadened-Gaussian Kubo Toyabe relaxation function. The observed short range order could be used to describe a new magnetic ground state, but a helical spin density wave with an incommensurate amplitude modulation cannot be ruled out. The sensitivity of μSR to the local magnetic field distribution in the vicinity of the quantum critical point (QCP) in $NbFe_2$ is clearly demonstrated via comparison with already published work. This suggests detailed measurements of the muon relaxation as the QCP is approached will reveal further details of the field distribution and fluctuations in $Nb_{1-y}Fe_{2+y}$.

Keywords: muon spin relaxation, quantum critical point, spin density wave
PACS: 76.75+i, 74.40.Kb, 75.30.Fv

1. Introduction

Detailed investigations of the phase diagram around quantum critical points (QCP) in correlated electron systems show rich behaviour including unconventional superconductivity and magnetic order. QCPs have been widely studied in heavy fermion systems [1] and their role in cuprates [2] and iron pnictide high-T_c [3] superconductors is still debated. Novel magnetic phases can also emerge [4] from a QCP. The $Nb_{1-y}Fe_{2+y}$ intermetallic is a particularly interesting material in which to investigate QCP behaviour since it displays a rich-magnetic phase diagram and quantum criticality in a *d*-band metal. The high temperature paramagnetic metal becomes a weakly ordered ferromagnet at relatively low temperatures in Nb-rich ($y < -0.02$) and Fe-rich ($y > 0.01$) compounds and the magnetic transition can be tuned to zero temperature at a doping of $y = -0.015$ [5]. Long-range antiferromagnetism (AF) or a spin density wave (SDW) have both been suggested to describe the magnetic ground state around criticality ($-0.02 < y < 0.01$) [5–12]. However ferrimagnetism in Fe-rich samples found by magnetic Compton scattering [13] and the current failure to detect the magnetic order by neutron scattering [5, 8] suggests further experiments are required to clarify the nature of the ground state. The existence of a ferromagnetic QCP would suggest that either the ferromagnetic state becomes discontinuous or a modulated SDW is formed [14].

Early magnetic studies of stoichiometric $NbFe_2$ [15] suggested a Pauli paramagnet ground state, but NMR work and magnetic investigations suggested an AF transition [6, 16] with a transition temperature, $T_N \sim 10$ K. Subsequent work suggested that the ordering resulted in a SDW [17] structure and that an applied field can suppress the ordering [18–20]. The AF or SDW ground state is characterised by a high magnetic susceptibility, non-Fermi liquid behaviour and the absence of magnetic remanence. Recently, significant efforts

Email address: marginedad@cardiff.ac.uk (D. Margineda)

have been made in order to further understand the nature of the apparently ambiguous magnetic ground state in $NbFe_2$ [5, 7–12]. Furthermore the possibility of competing and frustrated interactions can be postulated from the crystal structure since $NbFe_2$ crystallizes in the C14 hexagonal Laves phase with the magnetic Fe atoms (6h sites) forming two planar triangular kagome lattices, separated by linking Fe (2a sites) atoms in a hexagonal lattice and Nb atoms occupying interstitial sites, leading to numerous possible exchange pathways.

Theoretical studies have arrived at contradictory conclusions. The lowest energy magnetic ground state varies according to the method chosen in density functional theory calculations. Asano and co-workers [21] suggest that an antiferromagnetic ground state, and a "weak" as well as a "strong" ferromagnetic state have very similar ground state energies using the local-spin-density approximation. The more recent study of Subedi and Singh [22] found magnetic ground states governed by competing interlayer interactions, one which supports ferrimagnetism between 6h and 2a Fe atoms and another with no magnetic moment on 2a Fe sites and antiferromagnetic order. The antiferromagnetic interactions within the kagome lattice were found to be weak, which is supported by experiments [5], leading to the conjecture that geometric frustration is not associated with the quantum criticality. A new ferrimagnetic arrangement was also discovered in calculations using the generalised gradient approximation [23].

The Stoner enhancement factor, $1/(1-N(E_F)I)$, determined by experiment to be > 100 [8, 10], is associated with an unusually large exchange interaction, I. In this scenario any tiny increase in the density of states at the Fermi level $N(E_F)$, by doping should drive the magnetic ground state towards a ferromagnetic instability. Accordingly, calculations using the Korringa-Kohn-Rostoker electronic-structure method to study how chemical disorder affects the magnetic properties [24] using Moriya's theory of weak magnetism [25] suggest an unconventional band critical point as the most likely cause for a QCP, which is accessible by disorder due to alloying. Unlike the rigid-band approximation used in previous work, $N(E_F)$ increases in both the Fe and Nb rich alloys, thereby satisfying the Stoner criterion on both sides of the phase diagram.

Although an extensive amount of bulk magnetic, thermodynamic, transport and theoretical work has been performed, no definitive ground state has been unambiguously identified. Direct evidence of a modulated SDW has recently been reported using muon spin relaxation (μSR) [12]. Clear evidence of long range order in the doped samples was observed, the muon signal relaxed with an oscillatory behaviour which is a strong indication of static and ordered bulk magnetism. However the nature of the relaxation in the stoichiometric material is not as clear as the signal relaxes without any oscillatory behaviour making interpretation difficult. For $NbFe_2$, μSR is, in principle, able to differentiate between commensurate (AF) and incommensurate (SDW) magnetic order and weak ferromagnetism. Although correlation lengths are difficult to obtain directly from μSR, a phenomenological way to study short-range spin correlations in frustrated and/or magnetically disordered systems and spin glasses in the slow magnetic fluctuation regime has been proposed [26–31].

In this paper we present detailed μSR measurements of single crystalline stoichiometric $NbFe_2$, supported by d.c. and a.c. bulk magnetisation measurements to investigate the magnetic ground state. Using both zero field and longitudinal field μSR measurements we show that in our sample of stoichiometric $NbFe_2$ the observed magnetic order is static and short range, we describe the sensitivity of the ground state to stoichiometry. Comparison of our data to that already in the literature [12] suggests that muons are sensitive to the field distribution and fluctuations as the QCP is approached.

2. Bulk magnetisation

Magnetic data were taken in a commercial Physical Properties Measurement System (Quantum Design PPMS). All experimental data were taken with the magnetic field applied along the $c-$axis of the crystal. Initial magnetisation measurements as a function of temperature for both field-cooled and zero-field-cooled protocols show an obvious magnetic transition as shown in Fig. 1a.

Curie-Weiss (CW) like behaviour is observed down to the transition temperature, $T_N = 10.3$ K, indicated by a peak along with a bifurcation of the

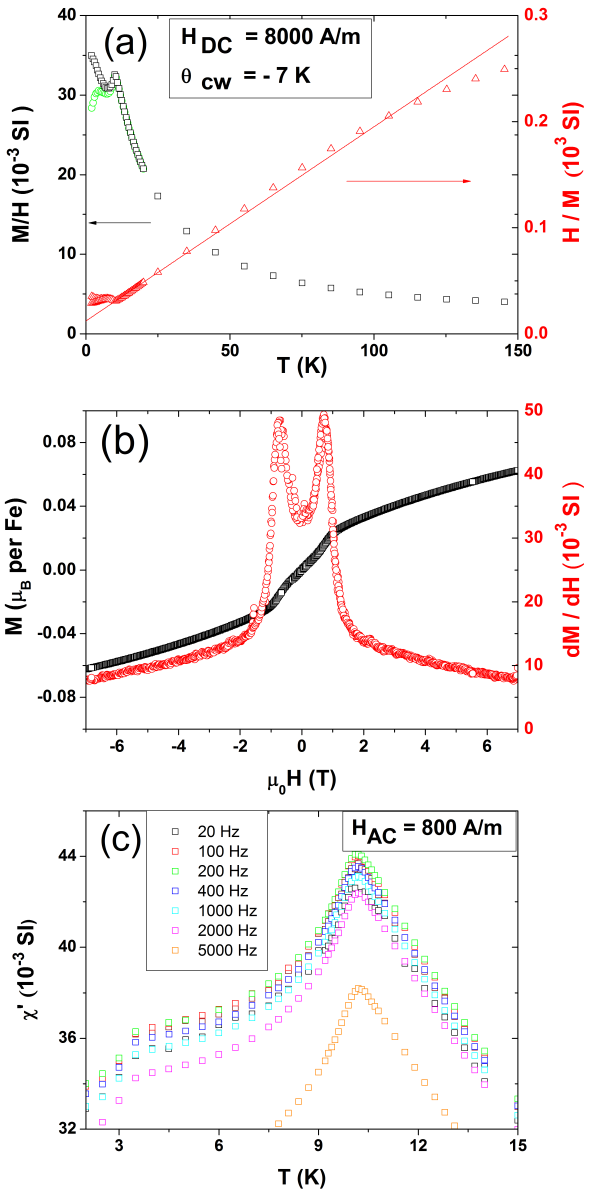

Figure 1: **AC and DC magnetisation:** (a) Temperature dependence of the field-cooled (black squares), zero field-cooled (green circles) susceptibility and inverse susceptibility (red triangles) showing a transition at $T_N = 10.3$ K. The inverse susceptibility displays approximately linear Curie-Weiss like behaviour, as is commonly observed in weak itinerant magnets [32]. (b) Magnetic isotherms (black squares) and susceptibility $\frac{dM}{dH}$ (red circles) at 2 K, indicating a critical field of $B_c \sim 0.7$ T. (c) Temperature-dependent a.c. susceptibility, no frequency-dependent behaviour is observed. Data are distorted by eddy currents above 1000 Hz.

field-cooled and zero-field-cooled magnetisation. This transition temperature is in good agreement with previously reported T_N values for stoichiometric samples of $NbFe_2$. Below T_N an "S" shaped magnetic field dependence exhibits a turning point at the critical field B_c necessary to suppress the observed order, (Fig. 1b). The derivative $\frac{dM}{dH}$ displays a critical field or maximum at $B_c \sim 0.7$ T, which is interpreted as a metamagnetic transition field, and is slightly higher than previously reported [5, 8, 16, 19].

The magnetisation below 100 K may be described in the local magnetic moment context with a CW behaviour. However, $NbFe_2$ is an itinerant paramagnet and the reason for the apparent CW behaviour is the temperature dependence of the spin-fluctuation amplitude [32]. In this scenario, the fact that the frustration parameter, $f = \frac{|\theta_{CW}|}{T_N}$ [33], is low may not be a reason to dismiss the geometrically frustrated Kagome lattice role in the magnetic ground state. However there is no frequency shift of the transition temperature in the susceptibility peak expected in a spin-glass system as shown in Fig. 1c. Above 1000 Hz the data are distorted by eddy currents induced in the metallic compound by the alternating field. No absorption is detected in the imaginary part $\chi''(\omega)$ (not shown). In our sample the magnetic transition is closer to a ferromagnetic instability than in previous work.

3. μSR, A local magnetic probe

μSR was chosen to investigate the nature of the magnetic ground state as it probes the local moment and fluctuations around the implanted muon site. The μSR technique occupies a broad time window, 10^{-9}-10^{-5}s, with which to observe spin fluctuations. In a μSR experiment, 100% spin polarised muons are implanted in the sample and then decay with a half-life of $\tau_\mu = 2.2$ μs. The muon polarisation, $P(t)$, is obtained from the asymmetry $A(t)$ in the positron counts as measured in backward (B) and forward (F) detectors with respect to the initial muon polarization: $A(t) = a_0 P(t) = \frac{F-\alpha B}{F+\alpha B}$, where a_0 is the initial asymmetry associated with a fully polarised muon ensemble, and α is an experimental parameter determined by the efficiency ratio of the F and B detectors and the position of the sample

with respect to those detectors. Any frequency (υ_i) of oscillations can be expressed by $\upsilon_i = \gamma_\mu |B_i|/2\pi$, where B_i is the average magnitude of the local field at the ith muon site and γ_μ is the muon gyromagnetic ratio. Any oscillatory signal observed in zero field μSR is direct evidence of long range magnetic order for a metallic system. If no oscillations are present the relaxation is a consequence of fluctuations and/or a distribution of local magnetic fields.

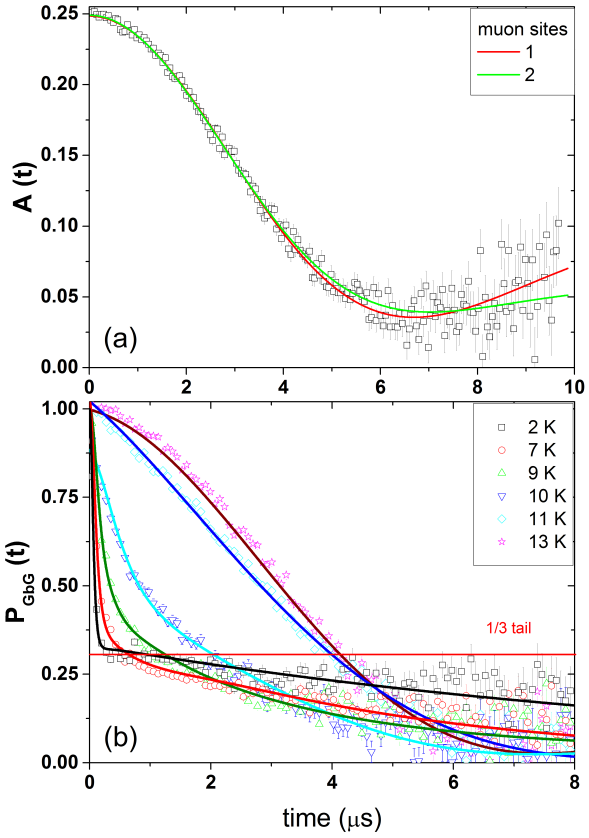

Figure 2: **Long times muon relaxation:** (a) Zero field μSR data as a function of temperature above T_N fitted with 1 and 2 muon sites. (b) Normalised long time muon spectra above and below T_N fitted to a GbG form as described in the text. The 1/3 tail level is shown by the red line.

The Dolly muon spectrometer at the continuous muon source at the Paul Scherrer Institute (PSI), Switzerland was used to study the magnetic ground state due to its high frequency resolution (and hence its ability to probe higher internal magnetic fields). The precise value of a_0 is dependent on the muon spectrometer. In the event that the muons find a stationary interstitial site in the sample (no hopping), then any relaxation in the observed $P(t)$ is a consequence of fluctuations around that muon site from nuclear or electronic spins. In the paramagnetic "motionally narrowed" regime, the muon relaxation in zero-field is dominated by nuclear spins which are static compared with the muon decay lifetime. As any magnetic transition is approached, and electronic spin-fluctuations slow down, electronic moments will dominate the relaxation because of the larger associated magnetic fields at the muon site.

On application of a transverse field in the paramagnetic phase above T_N, the muon polarization will oscillate around the applied field and the initial asymmetry, a_0, and the α parameter for the specific experiment can be experimentally obtained. For this experiment $a_0 = 0.25$. The non-relaxing background contribution to the muon asymmetry was measured in the zero field configuration and was found to be constant with temperature with a value of $a_{Ag} = 0.02$. Therefore the contribution from the sample, a_s, can be calculated from $A(t = 0) = a_s + a_{Ag} = 0.25$.

The sample was aligned with the muon polarisation along the $c-$axis. Firstly, zero field relaxation in the paramagnetic phase is discussed, where electron spins fluctuate faster than the muon time scale and the relaxation is dominated by weak and randomly oriented static nuclear moments. The local field at the muon sites at each coordinate i, B^i_{loc}, is distributed according to an isotropic Gaussian field distribution, with a standard deviation (Δ_G) and muons relax with a lineshape given by the well known Gaussian Kubo-Toyabe function (GKT) [34, 35]:

$$P_G(\Delta_G, t) = \left[\frac{1}{3} + \frac{2}{3}(1 - \Delta_G^2 t^2)\exp(-\frac{\Delta_G^2 t^2}{2})\right] \quad (1)$$

Δ_G is sometimes described as the local internal field because in an isotropic crystal $|\overrightarrow{B_{loc}}| = \sqrt{2}\Delta_G$. In the paramagnetic phase, the analysis of the measured muon relaxation should include the possibility of numerous interstitial muon stopping sites so that the field distribution below the ordering temperature can be understood. An extensive study of the interstitial muon sites in the paramagnetic phase of $NbFe_2$ was performed in the work of Crook [20]. The muon relaxation was described by the distribution of the Nb and Fe ions around the implanted muons, which are distinguishable because of their different nuclear moments. Around

the muon site the local environment can be described by the elements surrounding it, three possible (Nb-Fe) nearest neighbour coordinations of 4-0, 3-1 and 2-2 are possible. Simulations of the nuclear field distribution due to Gaussian distributed atomic moments for each of these site coordinations result in the following Δ_G values: 0.199, 0.39 and 0.48 μs^{-1} respectively. In the work of Crook, a single GKT relaxation with a field width of 0.284 μs^{-1} was associated with a single muon stopping site at the 4-0 position [20].

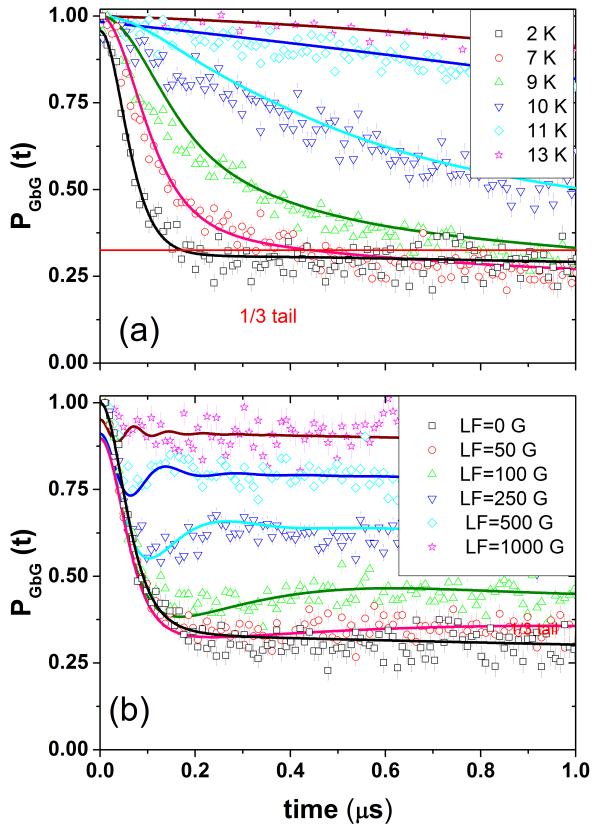

Figure 3: **Normalised short times muon relaxation:** (a) Short time muon spectra above and below T_N fitted to a GbG form as described in the text. (b) Decoupling of the internal local field is shown by the application of a longitudinal field. The associated fits are described in the text.

In this study, we also find that we can fit the data with one muon site in the paramagnetic regime as shown in Fig. 2a. It is important to note that the site allocation is more difficult to perform at PSI in this sample as the time scale only extends to 10 μs^{-1}. The average nuclear field we found is $\Delta_G/\gamma_\mu = 0.29$ mT or $\Delta_G = 0.253$ μs^{-1}. This is close to the value found in the previous work. The difference between the measured and the calculated values can be be explained and simulated [20] by site mixing (anti-site disorder) which would also have an effect on the local field distribution in the ordered regime.

The magnetic phase was analysed with zero field μSR above and below T_N. The Gaussian relaxation from the nuclear contribution dominates above T_N but below the transition the relaxation is modified by the magnetic order with a fast muon depolarisation as shown Fig. 2b. Several scenarios for order can be distinguished by the nature of the relaxation below T_N. Specifically if oscillations were observed this would signify long range order and may signify a modulated SDW [34]. However we see no oscillations in $P(t)$, in agreement with recent work [12]. In the absence of oscillations, μSR can distinguish two possible cases [35]. In the fast fluctuation or motional narrowing limit, an exponential decay characterises the muon depolarisation [36], and the relaxation rate contains information about both magnetic fluctuations and field-distribution widths. In the other case, when fluctuations are slow, the magnetic field at the muon sites can be considered quasi-static. These scenarios can be distinguished by the application of a longitudinal field (along the direction of the muon polarization). The absence of oscillations and a relaxing tail at $\sim 1/3$ of the muon polarisation observed in Figs. 2b and 3a below 5 K suggest slow spin fluctuations of randomly orientated quasi-static fields, with a relaxation lineshape reminiscent of a Kubo-Toyabe (KT) function given by Eq. 1. In the "static" approximation, the long time muon asymmetry is independent of time and equal to the 1/3 term in Eq. 1. This is known at the "1/3 tail" region. However the presence of slow fluctuations can further depolarise the "1/3 tail" region. KT functions in magnetically ordered single-crystalline samples are often used to fit the muon relaxation in disordered and/or frustrated magnetic phases with slow spin dynamics. In such cases, relaxation is dominated by randomly orientated magnetic fields at the muon sites.

Densely packed magnetic moments can generate a Gaussian field distribution at muon sites whilst systems with dilute magnetic impurities such as

canonical spin glass may produce a Lorentzian field distribution. Both cases present a distinctive dip in the muon asymmetry and a "1/3 tail". However, neither can fit the muon spectra we measure for $NbFe_2$, ruling out these simple interpretations for the magnetic ground state. Moreover a limited number (3) of combined KT representing different possible muon sites or 2 simple exponentials cannot model the data. We have therefore utilised a phenomenological Gaussian-broadened GKT function (GbG), introduced by Noakes *et al* [26]., to explain several dense magnetic systems, to fit our data. In this model, the single isotropic Gaussian field distribution $D_G(B^i_{loc},\Delta_G)$ assumed in the GKT function of Eq. 1, is replaced by a distribution of Gaussian distributions D_{GBG} of width ρ centred on Δ_0 and with a standard deviation $R_b\Delta_0$. This lineshape is sometimes used to describe systems with static dense magnetic moments, but correlated only over a short range, with examples of its use being found in the quantum spin-ice $Yb_2Ti_2O_7$ [37] and the $5d$ hyperkagome lattice $Nd_4Ir_3O_8$ [29]. The GbG field distribution is:

$$D_{GbG}(B^i_{loc}) = \int_{-\infty}^{\infty} D_G(B^i_{loc},\Delta_G)\rho(\Delta_G,\Delta_0,R_b)d\Delta_G \tag{2}$$

where

$$\rho(\Delta_G,\Delta_0,R_b) = \frac{1}{\sqrt{2\pi}}\frac{1}{R_b\Delta_0}\exp\left[-\frac{(\Delta_G-\Delta_0)^2}{2(R_b\Delta_0)^2}\right] \tag{3}$$

The resultant muon depolarisation is the analytical solution of the integral Fourier transform of Eq. 2: Although the integral runs only over positive Δ_G values, it was extended to $-\infty$ to simplify to the following solution [35]:

$$P_{GbG}(\Delta_0,R_b,t) = \frac{1}{3}\exp(-\frac{2}{3}\nu t) + \frac{2}{3}\left(\frac{1}{1+R_b^2\Delta_0^2t^2}\right)^{\frac{3}{2}} \left(1-\frac{\Delta_0^2t^2}{1+R_b^2\Delta_0^2t^2}\right)\exp\left[-\frac{\Delta_0^2t^2}{2(1+R_b^2\Delta_0^2t^2)}\right] \tag{4}$$

In the slow fluctuation limit, the magnetic fluctuation rate ν depolarises the "1/3 tail" at long relaxation times. The muon depolarisation (Eq. 4) describes an effective local field $\Delta^2_{eff} = \Delta_0^2 + R_b^2\Delta_0^2$ and evolves from a Gaussian KT when $R_b = 0$ (displaying a distinctive dip in the data) towards a monotonic relaxation when $R_b \simeq 1$. The data in Figs. 2b and 3a were best fit to the GbG function using the Musrfit software [38] between 1.8 K and T_N with a maximum effective local field at 2 K ($\frac{\Delta_{eff}}{\gamma_\mu} = 0.014$ T) and $R_b \simeq 1$.

The distribution of internal fields $\rho(\Delta_G)$ (Eq. 3.) is plotted as a function of Δ_G for various different temperatures in Fig. 4a. The mathematical approximation in Eq. 4 entails $\rho(\Delta_G) \neq 0$ for $\Delta_G < 0$ if $R_b \simeq 1$. As Δ_G is an absolute value the equation is redefined:

$$\rho(\Delta_G) \equiv \begin{cases} \rho(\Delta_G)+\rho(-\Delta_G) & \Delta_G > 0 \\ 0 & \Delta_G < 0 \end{cases}$$

The randomly-orientated internal fields are evenly distributed from 0 to the fitted effective local field Δ_{eff} (shown by the arrow in Fig. 4a). The inset shows Δ_{eff} measuring with the transition temperature and a guide to the eye.

The quasi-static nature of the internal fields may be confirmed by longitudinal field (LF) μSR. In order to analyse and to test the distribution of fields described previously we discretised the D_{GBG} and fitted the data to a sum of single gaussian distributions, $D_G(\Delta_G)$, according to the weighting obtained from Fig. 4a. 17 Gaussian distributions give a good fit for the ZF-μSR and were used to fit the longitudinal field data shown in Fig. 3b.

The LF muon asymmetry spectra repolarised when fields are applied, as expected from quasi-static internal fields. The effective local field at the muon sites can be estimated from the maximum field where slight wiggles can still be observed, $\frac{\gamma_\mu B^{max}_{ext}}{\Delta_{eff}} \sim 5-10$ [34, 35]. In our case, $B^{max}_{ext} = 0.1$ T gives a $\frac{\Delta_{eff}}{\gamma_\mu} \sim 0.01-0.02$ T, in the same order as values obtained from the ZF μSR measurement. The scaling method from Rauch *et al* [12]., may be used to estimate the local magnetisation. The local magnetisation is calculated assuming it scales to the effective internal fields in the same way as the bulk magnetisation of the ferromagnetic doped samples scales to the muon oscillation frequency (Ω_B in that work). We obtain a local magnetisation of $M \approx 0.0075\mu_B$/Fe.

The magnetic relaxation rate ν increases slightly when the temperature approaches T_N but remains in the slow fluctuation limit: $\nu < \Delta_{eff}$. When the longitudinal field is applied as can be seen in Fig.

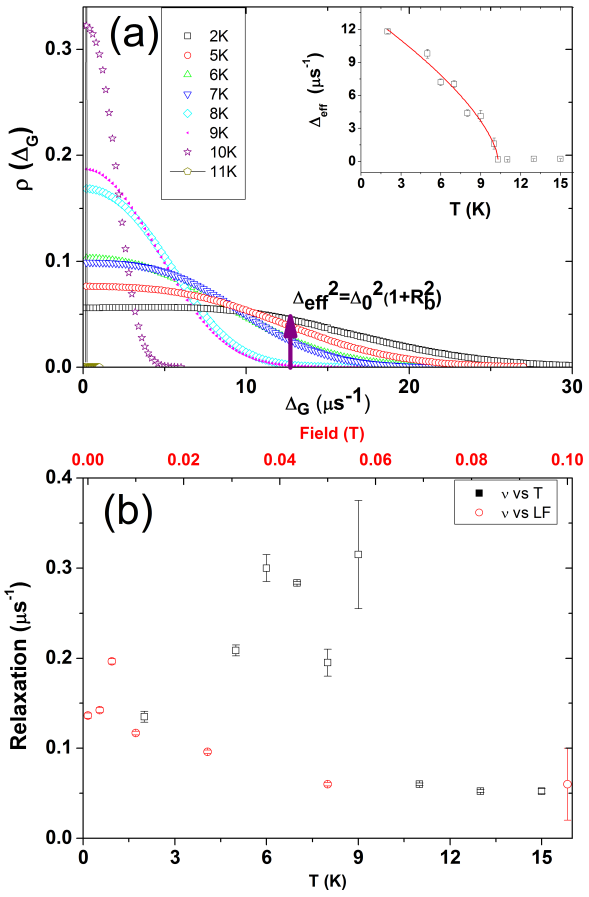

Figure 4: **Muon parameters:** (a) Distribution of the local internal fields as a function of temperature from 0 to Δ_{eff}. The inset shows the temperature dependence of effective local fields below T_N, the line is a guide to the eye. (b) Fluctuations as a function of temperature (black squares) and field at 2 K (red circles).

4b the relaxation rate is lower than 0.2 μs^{-1} at 2 K at all fields. The nature of the magnetically ordered phase for our sample of $NbFe_2$ does not uniquely describe a simple spin density wave, as no oscillations are seen in the muon spectra in agreement with previous work [12]. In an incommensurate SDW phase, muons could depolarise according to a Bessel function, behaviour which cannot describe the measured relaxation. However the quasi-static nature of randomly orientated internal fields were confirmed by our experiments.

In ZF-μSR, two relaxation processes are observed: a fast depolarisation due to the randomly-orientated static fields; and a slowly depolarising 1/3 tail region, corresponding to slow fluctuations of the local fields. In LF-μSR, muon decoupling is observed by applying magnetic fields as expected from quasi-static fields. The homogenous distribution of internal fields Δ_{eff} is described by the GBG relaxation in the ZF data and by an equivalent sum of Gaussian relaxations for the LF data. This behaviour could be induced by short-range correlations. The correlation length has previously been associated to the R_b parameter [31] where values close to 1 make the correlation length short enough to be 'seen' as randomly-orientated magnetic moments by the muons. In our case the value of R_b is always around 1. In a helical SDW phase the moment orientation rotates from one unit cell to another and the muons will be affected by a broad distribution of fields as we observe for incommensurate order and apparent randomness could emerge at the muon sites. The subtle change of muon relaxation between our work and that of Rauch *et al* [12]., for at and just off stoichiometry as the QCP is approached suggests the importance of site mixing and that muon relaxation can be used to study the local magnetic environment in detail as the material is tuned towards the QCP. Importantly the data presented in this paper and previous [12] work suggest that application of longitudinal fields may reveal changes in the field distribution and fluctuation rates as the QCP is approached.

4. Conclusions

The SDW magnetic phase reported around criticality was studied in stoichiometric $NbFe_2$ by bulk magnetic techniques and the local probe μSR. The transition temperature found by all the techniques is consistent with the Neel temperature reported at stoichiometry [5, 8, 10, 11]. However our sample has a higher critical field, in the magnetically ordered phase.

A long range magnitude modulated SDW order cannot be confirmed by μSR, however the static nature of the magnetic field is clearly observed below the transition. Although fluctuations at 2 K remain in the slow fluctuation regime. The μSR data were fitted with a phenomenological GbG Kubo-Toyabe function. The muon relaxation is due to randomly-orientated static fields with magnitudes homogeneously distributed from 0 to an effective field, Δ_{eff}, equivalent to $M \sim 0.0075\mu_B$/Fe.

Similar results by Rauch et al.[12] are explained as a magnitude modulated SDW with a large correlation length but the absence of oscillations and the distribution of the randomly-orientated quasi-static fields suggest a magnetic phase controlled by short-range correlations and only a SDW with a helical and incommensurate amplitude modulation may explain our results.

The sensitivity of μSR to the distribution of local magnetic fields in the vicinity of the QCP is clearly demonstrated and further investigation in the weak AFM region could shed some light on the magnetic ground state and fluctuations as the QCP is approached.

5. Aknowledgments

The authors would like to thank G. Stenning for support with AC susceptibility measurements. This work was supported by EPSRC (EP/L019760/1) of the UK.

6. References

[1] Q. Si and F. Steglich, Science **329**, 1161 (2010).
[2] D. v. d. Marel, H. J. A. Molegraaf, J. Zaanen, F. Nussinov, Z.and Carbone, A. Damascelli, H. Eisaki, M. Greven, P. H. Kes, and M. Li, Nature **425**, 271 (2003).
[3] G. Giovannetti, C. Ortix, M. Marsman, M. Capone, J. van den Brink, and J. Lorenzana, Nat. Commun. **2**, 398 (2011).
[4] Y. Tokiwa, J. J. Ishikawa, S. Nakatsuji, and P. Gegenwart, Nat. Mater. **13**, 356 (2014).
[5] D. Moroni-Klementowicz, M. Brando, C. Albrecht, W. Duncan, F. M. Grosche, D. Grüner, and G. Kreiner, Phys. Rev. B **79**, 224410 (2009).
[6] Y. Yamada and A. Sakata, J. Phys. Soc. Japan **57**, 46 (1988).
[7] D. Moroni-Klementowicz, R. Burrell, D. Fort, and M. Grosche, Physica B: Cond.Mat. **359-361**, 80 (2005).
[8] M. Brando, D. Moroni-Klementowicz, C. Albrecht, and F. M. Grosche, Physica B: Cond. Mat. **378-380**, 111 (2006).
[9] R. Sato Turtelli, J. Sinnecker, R. Grössinger, a. Penton-Madrigal, and E. Estevez-Rams, J. Magn. Magn. Mat. **316**, 492 (2007).
[10] M. Brando, W. Duncan, D. Moroni-Klementowicz, C. Albrecht, D. Grüner, R. Ballou, and F. M. Grosche, Phys. Rev. Lett. **101**, 026401 (2008).
[11] S. Friedemann, M. Brando, W. Duncan, A. Neubauer, C. Pfleiderer, and F. M. Grosche, Phys. Rev. B **87**, 024410 (2013).
[12] D. Rauch, M. Kraken, F. J. Litterst, S. Süllow, H. Luetkens, M. Brando, T. Förster, J. Sichelschmidt, A. Neubauer, C. Pfleiderer, et al., Phys. Rev. B **91**, 174404 (2015).
[13] T. D. Haynes, I. Maskery, M. W. Butchers, J. a. Duffy, J. W. Taylor, S. R. Giblin, C. Utfeld, J. Laverock, S. B. Dugdale, Y. Sakurai, et al., Phys. Rev. B **85**, 115137 (2012).
[14] A. V. Chubukov, C. Pepin, and J. Rech, Phys. Rev. Lett. **92**, 147003 (2004).
[15] M. Shiga and Y. Nakamura, J. Phys. Soc. Japan **56**, 4040 (1987).
[16] M. Kurisu, Y. Andoh, and Y. Yamada, Physica B: Condensed Matter **237-238**, 493 (1997).
[17] Y. Yamada, H. Nakamura, Y. Kitaoka, K. Asayama, K. Koga, A. Sakata, and T. Murakami, J. Phys. Soc. Japan **59**, 2976 (1990).
[18] R. Crook, M R. Cywinsky, Hyperfine Interact. **85**, 203 (1994).
[19] M. R. Crook and R. Cywinksi, J. Magn. Magn. Mater. **144**, 71 (1995).
[20] M. Crook, Ph.D. thesis, The University of Reading (1995).
[21] S. Asano and S. Ishida, J. Phys. Cond. Mat. **1**, 8501 (1989).
[22] A. Subedi and D. J. Singh, Phys. Rev. B. **81**, 024422 (2010).
[23] D. A. Tompsett, R. J. Needs, F. M. Grosche, and G. G. Lonzarich, Phys. Rev. B **82**, 155137 (2010).
[24] A. Alam and D. D. Johnson, Phys. Rev. Lett. **107**, 206401 (2011).
[25] B. P. Neal, E. R. Ylvisaker, and W. E. Pickett, Phys. Rev. B **84**, 085133 (2011).
[26] D. R. Noakes and G. M. Kalvius, Phys. Rev. B **56**, 2352 (1997).
[27] D. R. Noakes, J. Phys. Cond. Mat. **11**, 1589 (1999).
[28] P. Dalmas de Réotier, V. Glazkov, C. Marin, A. Yaouanc, P. Gubbens, S. Sakarya, P. Bonville, A. Amato, C. Baines, and P. King, Physica B **374-375**, 145 (2006).
[29] R. Dally, T. Hogan, A. Amato, H. Luetkens, C. Baines, J. Rodriguez-Rivera, M. J. Graf, and S. D. Wilson, Phys. Rev. Lett. **113**, 247601 (2014).
[30] D. E. MacLaughlin, P.-C. Ho, L. Shu, O. O. Bernal, S. Zhao, A. A. Dooraghi, T. Yanagisawa, M. B. Maple, and R. H. Fukuda, Phys. Rev. B **89**, 144419 (2014).
[31] A. Yaouanc, A. Maisuradze, and P. Dalmas De Réotier, Phys. Rev. B **87**, 134405 (2013).
[32] T. Moriya, *Spin Fluctuations in Itinerant Electron Magnetism*, Springer Series in Solid State Sciences (Springer-Verlag, 1985).
[33] A. P. Ramirez, Annu. Rev. Mater. Sci. **24**, 453 (1994).
[34] S. Lee, S. Kilcoyne, and R. Cywinski, eds., *Muon Science. Muons in Physics, Chemistry and Materials* (Scottish Universities Summer School in Physics and Institute of Physics Publishing, Bristol and Philadelphia, 1998).
[35] A. Yaouanc and P. Dalmas de Réotier, *Muon Spin Rotation, Relaxation and Resonance: Applications to Condensed Matter* (Oxford University Press, Oxford, 2011).
[36] M. J. Graf, S. M. Disseler, C. Dhital, T. Hogan, M. Bojko, A. Amato, H. Luetkens, C. Baines, D. Margineda, S. R. Giblin, et al., Journal of Physics: Conference Series **551**, 012020 (2014).
[37] J. A. Hodges, P. Bonville, A. Forget, A. Yaouanc,

P. Dalmas De Réotier, G. André, R. M, K. K, C. Ritter, P. C. M. Gubbens, et al., Phys. Rev. Lett. **88**, 077204 (2002).
[38] *http://lmu.web.psi.ch/musrfit/technical/index.html*.